JOURNAL OF CATALYSIS 157, 201–208 (1995)

# A Reaction Calorimetric Investigation of the Hydrogenation of a Substituted Pyrazine

Ralph N. Landau,[1] Utpal Singh, Frank Gortsema, Yongkui Sun, Susan C. Gomolka, Thientu Lam, Mauricio Futran, and Donna G. Blackmond[2]

*Merck & Company, Inc., P.O. Box 2000, Rahway, New Jersey 07065*

Received September 27, 1994; revised May 9, 1995; accepted June 23, 1995

**Reaction calorimetry was the primary tool in investigations of the liquid-phase hydrogenation of a substituted pyrazine compound carried out over supported Pd catalysts. In addition to providing information about gas–liquid mass transfer limitations, calorimetric measurements provided a kinetic analysis of how product selectivity in this consecutive reaction network may be tuned by changing reaction conditions. Concentration profiles developed from fitting the heat flow data to a first-order model were compared with analytical measurements of concentration, demonstrating the utility of combining independent measurements of reaction progress as a means of assessing the validity of a kinetic model.** © 1995 Academic Press, Inc.

## INTRODUCTION

A significant number of the heterogeneous catalytic reactions carried out in the production of fine chemicals and pharmaceuticals involve the selective hydrogenation of complex organic molecules (1). Selectivity concerns in these reactions may focus on enhancing the hydrogenation of one functional group in a molecule containing different functional groups including halides or nitro groups, or it may involve the partial hydrogenation of a molecule containing several unsaturated bonds including C=C, C=O, or C=N bonds. In each case, careful choice of the type of metal, the support, and any additives may all affect the ultimate product selectivity. In addition, the reaction conditions themselves may be used as a means of controlling selectivity, especially in cases where diffusion limitations present a concern (2, 3).

In the present investigation, a substituted pyrazine compound is hydrogenated to the corresponding piperazine over supported Pd:

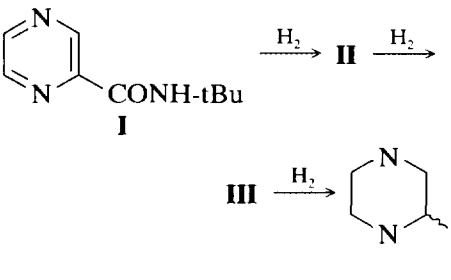


[1]

The organic substrate, pyrazine-2-*tert*-butylcarboxamide (**I**), is an intermediate in the production of an anti-AIDS drug currently under investigation in these laboratories (4). The reaction involves three consecutive hydrogenation steps of the pyrazine ring while preserving the amide group conjugated with the ring. The three-phase reaction is carried out under mild conditions over Pd/C catalysts.

This investigation uses heat flow reaction calorimetry as the primary tool for exploring both the kinetics of the reaction network and gas–liquid diffusion limitations. An energy balance around a well-stirred batch reactor under isothermal conditions shows that the heat flow is proportional to the reaction rate,

$$q_r = V_r \sum_i \Delta H_{rxn,i} \frac{dC_i}{dt} \qquad [2]$$

where $q_r$ is the heat flow, $V_r$ is the volume of the reactor contents, and $(dC_i/dt)$ is the rate and $\Delta H_{rxn,i}$ is the heat of the $i$th reaction, respectively. Equation [2] assumes that physical thermal effects such as heats of mixing are negligible compared to the heats of reaction; an assumption that holds for low viscosity systems and can be easily verified in each case. This work demonstrates how heat flow data serve as a measure of the reaction progress and may be used as an independent complement to analytical concentration data in developing and testing kinetic models of the reaction network.

[1] Present address: Sandoz Pharmaceutical Corporation, 59 Route 10, East Hanover, NJ 07936-1080.

[2] To whom correspondence should be addressed at Institut für Technische Chemie, Universität Essen, D-45117 Essen, Germany. E-mail: donna.blackmond@uni-essen.de.



0021-9517/95 $12.00
Copyright © 1995 by Academic Press, Inc.
All rights of reproduction in any form reserved.

## EXPERIMENTAL

### *Catalysts and Catalyst Characterization*

Two carbon-supported Pd catalysts of different metal loadings (5% Pd, Engelhard Escat-112, and 20% Pd, Johnson-Matthey Pearlman's type) were used in this study. Both catalysts were prepared as $Pd/(OH)_2$ on carbon with a water content near 50 wt%. The catalysts were used without pretreatment. Reduction to the active Pd surface takes place rapidly *in situ* during the catalytic hydrogenation reaction (5).

Catalysts were characterized by temperature programmed reduction (TPR) and by pulse chemisorption of CO using an Altamira Instruments AMI-1 automated temperature programmed system. For TPR experiments, 10% $H_2$ in Ar (Matheson) was passed over the catalyst at 100 cc/min while the temperature was ramped from 298 to 773 K at 10 K/min. Pulse chemisorption measurements were carried out using 100 $\mu$l pulses of CO (99.9%, Matheson) in He at 100 ml/min until saturation coverage was achieved.

### *Organic Reagents*

The organic substrate, pyrazine-2-*tert*-butylcarboxamide (**I**), was produced in-house at Merck. Standard samples for GC calibration of the product piperazine compound (**IV**) were also prepared at Merck. Standards for the intermediate species **II** and **III** were not available. The solvent employed was *n*-propanol with the organic substrate at concentrations of between 40–200 g/liter (ca. 0.2–1 *M*). The catalyst/organic substrate ratio was 0.095–1.25% Pd on a w/w basis.

### *Gas–Liquid Mass Transfer Measurements*

Gas–liquid mass transfer coefficients, $K_La$, were measured in the reaction calorimeter by a dynamic method described previously (3, 6, 7) which measures the rate of dissolution of hydrogen in the liquid phase (solvent and organic substrate). Briefly, hydrogen at 593 kPa was introduced to the degassed reactant mixture in the absence of the catalyst, and the subsequent pressure drop was monitored during agitation. The rate of gas–liquid mass transfer (7) is given as a function of time and the initial and final pressures, $P_i$ and $P_f$, the vapor pressure $P_0$ of the mixture at reaction temperature, and the pressure at any time $t$, $P$:

$$\frac{P_f - P_0}{P_i - P_0} \ln\left[\frac{P_i - P_f}{P - P_f}\right] = K_La \times t. \qquad [3]$$

The total pressure decrease until equilibrium is established also yields the solubility of hydrogen in the solution under the conditions of the experiment. From these parameters the maximum rate of hydrogen delivery from the gas to the liquid may be determined by

$$r_{max} = K_La \times C^{sat.P_f}, \qquad [4]$$

where $C^{sat.P_f}$ is the solubility of hydrogen at the final pressure of the experiment.

### *Catalytic Reactions*

Catalytic reactions were carried out in the liquid phase using a fully automated reaction calorimeter (Mettler RC1) with reaction volume of either 150 or 500 ml. Agitation speeds between 100–1000 rpm were employed. Isothermal reactions were carried out at temperatures ranging from 293–343 K under constant hydrogen pressure of 593 kPa fed from either or both super- and subsurface (with 5 $\mu$m diffuser) gas lines. Some reactions were also carried out using a 300 ml stirred autoclave (Parr Instruments).

Heat flow caorimetry was used to give an energy balance around the outer surface of the reactor at any time during all reaction experiments,

$$q_r = UA(T_r - T_j) + mC_p\, dT_r/dt, \qquad [5]$$

where the instantaneous heat flow is given by $q_r$, $U$ is the overall heat transfer coefficient, $A$ is the wetted area, $T_r$ is the reactor temperature, $T_j$ is the jacket temperature, $m$ is the mass of the reactor contents, and $C_p$ is the heat capacity of the reactor contents. A calibration experiment imposing known $q_r$ values on the system was performed to solve for the unknown quantities $U$ and $C_p$ as has been described previously (8, 9) and will be summarized briefly here. A precision heating probe providing a known heat flow as first immersed in the reactor contents while the calorimeter maintained isothermal conditions. Thus with $dT_r/dt$ equal to 0, and $q_r$ equal to the power rating of the probe, Eq. [5] was used to solve for the heat transfer coefficient, $U$. Next, a short temperature ramp of the jacket was carried out under conditions where $q_r$ was equal to 0, which set the heat flow through the reactor wall equal to the enthalpy accumulation, allowing solution for $C_p$ in Eq. [5]. This procedure was typically carried out before initiating reactions and after reaction was complete to account for changes in these properties with extent of reaction. Using these two calibration endpoints, the energy balance shown in Eq. [5] is evaluated by appropriately varying the properties $U$ and $C_p$ over the course of the reaction. Heat accumulated in the agitator or other reactor inserts were accounted for in the calorimeter heat balance but are omitted in the above equation for the sake of brevity.

### *Kinetic Modeling*

Heat flow values were recorded continuously (every 6 s) as a function of time during the reaction. Data from this

large set of $(q_r, t)$ points for each experiment were averaged to give a data set of tractable size for use in modeling. For quantitative analysis of heat flow data, a baseline value for heat flow, $q_b$, was recorded prior to initiation of the reaction, and this value (about 0.4 W) was subtracted from the values recorded during the reaction. The accuracy of the heat flow measurements is estimated to be approximately ±0.1 W. Kinetic modeling was carried out using heat flow data from zero conversion to the conversion at which the heat flow decayed to 0.5 W.

Since no products other than those in the reaction network were observed under the conditions employed, the mass balance for the system at any time $t$ is given by

$$C_{I_0} = C_I + C_{II} + C_{III} + C_{IV}, \quad [6]$$

where $C_{I_0}$ is the initial substrate concentration and the $C_i$'s are the concentration of each species at time $t$. A series of first order consecutive reactions was chosen as a simple model of the reaction network. From Eq. [1], the corresponding heat flow equation for this model is

$$q_r = [\Delta H_{rxn,1} k_1 C_I + \Delta H_{rxn,2} k_2 C_{II} + \Delta H_{rxn,3} k_3 C_{III}] V_r. \quad [7]$$

Standard heats of reaction for each step were obtained from molecular modeling as described below. These $\Delta H^\circ_{rxn}$ values were used without correction over the temperature range 293–313 K employed in these experiments, since the error was less than 0.5 kcal/mol, determined from experimental heat capacities for the reactant and product mixtures. The temperature-dependent rate constants are given by an Arrhenius expression $k = A \exp(-E_a/k_B T)$. The experimental heat flow vs time curves were used to solve Eq. [6] and [7] for all three isothermal reactions simultaneously to give the preexponential factors $A_i$ and activation energies $E_{ai}$ for each step as well as the concentration profiles for each species as a function of reaction time. Microsoft Excel Solver was used to compile model heat flow curves with an average percent error of less than 7% compared to the experimental heat flow curves. Although similar solutions were obtained using different initial guesses for the kinetic parameters, the solution presented may represent a local rather than a global minimum.

### *Molecular Modeling*

Molecular modeling of the consecutive hydrogenation of **I** was carried out to estimate the heat of reaction for each step to use in the kinetic modeling of the heat flow curves. A semiempirical quantum mechanical package (CAChE Group, Inc.), was used to calculate heats of formation of the four compounds in the reaction network. Molecular modeling proposed the most stable of several possible structures for species **II** and **III**. The structure of each molecule was first optimized by molecular mechanics to minimize steric energy, followed by optimization of electronic properties by MOPAC using the AM1 (10).

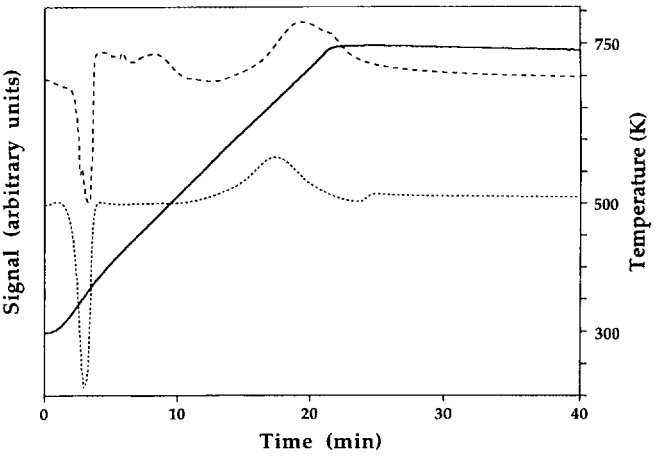


FIG. 1. Temperature programmed reduction spectra for two Pd/C catalysts employed in these reaction studies. 20 wt% Pd (long dashes); 5 wt% Pd (short dashes); Temperature ramp (solid line).

### *Sample Analysis*

Samples were obtained manually as the reaction progressed and analyzed by LC (Thermo Separation) using a Zorbax RXC8 column with a 2:98 water:acetonitrile mobile phase (UV detector set at 254 nm) and by GC and GC/MS (Hewlett–Packard) with an HP-5 column. The compounds **I**, **II**, and **III** could be detected by either GC or LC, and product **IV** was analyzed by GC and GC/MS. The analytical data for compounds **I** and **II** is reported as a sum of the two. A reliable analytical method for determining concentration of **II** was not available due to rapid oxidation of **II** back to **I** once samples were exposed to air.

## RESULTS AND DISCUSSION

### *Catalyst Characterization*

TPR spectra for both catalysts are shown in Fig. 1. Desorption of hydrogen was observed as a negative peak near 345 and 365 K for the 5 and 20% Pd catalysts, respectively, which is characteristic for supported Pd and is attributed either to weakly adsorbed or absorbed hydrogen (11). This feature of the TPR curve suggests that a portion of the Pd surface was already reduced in the first few minutes of exposure to hydrogen at ambient temperature before data collection could begin, supporting studies which have shown that Pd catalysts may be reduced from salts such as $Pd(OH)_2$ even at subambient temperatures (5, 11). Broad, higher temperature peaks for hydrogen uptake were observed near 495 and 700–773 K for the 20% Pd sample and near 600–675 K for the 5% Pd sample, although any

TABLE 1

**Reaction Data for Conversion of I under Diffusion Limitations**

| Catalyst | Dispersion (%) | Pd/substrate (wt/wt) | $T$ (K) | Agitation speed (rpm) | Reaction time for 95% conversion **I** → **IV** (min) |
|---|---|---|---|---|---|
| JM-20 | 6 | 0.0125 | 353 | 400 | 350 |
| JM-20 | 6 | 0.0076 | 343 | 800 | 330 |
| ES-5 | 10 | 0.0038 | 343 | 800 | 330 |
| ES-5 | 10 | 0.0038 | 343 | 1000 | 100 |

surface Pd produced from reduction at these high temperatures is unlikely to be important for the low temperature catalytic reactions under study. CO pulse chemisorption measurements showed that the 20% Pd catalyst had a dispersion of about 6% while the 5% Pd catalyst was about 10% dispersed. This indicates that the catalyst containing four times as much Pd for a given weight of catalyst actually exhibited closer to twice the concentration of surface Pd sites on that same per weight catalyst basis. The relatively low dispersion of this type of catalyst is a consequence of its preparation method, which yields particles of $Pd(OH)_2$ easily reducible to the active state under the mild conditions of the liquid-phase hydrogenation reactions in which they are typically used (5), thus obviating the need for a separate, more rigorous, pretreatment step.

*Investigation of Bulk Hydrogen Diffusion Limitations*

The hydrogenation of pyrazine ring of pyrazine-2-*tert*-butylcarboxamide (**I**) to piperazine-2-*tert*-butylcarboxamide (**IV**) was accomplished in consecutive hydrogenation steps without observation of any side reactions involving the C=O group of the amide under any conditions. However, our initial reaction results as shown in Table 1 suggested that the intrinsic kinetics of the system might be masked by other rate processes. The time required for 95% conversion of **I** to **IV** for reactions carried out over two different catalysts under different reaction conditions decrease as expected with increases in the amount of catalyst and the reaction temperature. The variable which influenced reaction rate to the greatest extent was agitation speed, suggesting that under the conditions employed the rate of the reaction was limited by the rate of gas–liquid mass transfer.

Other studies by our group have illustrated, using heat flow calorimetry, the effect of agitation speed on the observed rate for diffusion limited reactions (3). Figure 2 gives the results of a reaction in which the agitation speed was varied in steps from 100 to 1000 rpm over the course of the reaction. Since heat flow is proportional to reaction rate, monitoring the heat flow over the course of the experiment gives a continuous measure of the rate. At very low agitation speeds, the reaction rate was correspondingly low. Each increase in agitation speed up to 750 rpm, at which point the reaction was essentially complete, resulted in an increase in reaction rate as indicated by each sharp increase in the heat flow curve. This suggests that the availability of hydrogen to the catalyst increased as more effective agitation increased the rate of gas–liquid mass transfer of hydrogen.

While monitoring of the heat flow profile as a function of agitation speed during the reaction can provide a qualitative picture of the conditions under which bulk mass transfer of hydrogen may be rate limiting, a quantitative analysis of the regime of bulk hydrogen diffusion limitations may be made by measurements of the mass transfer coefficient, $K_La$, as described in the Experimental Section. Table 2 shows that $K_La$ was a strong function of the agitation speed, increasing by more than two orders of magnitude as the agitation speed increased from 400 to 1000 rpm.

The maximum rate of gas–liquid mass transfer calcu-

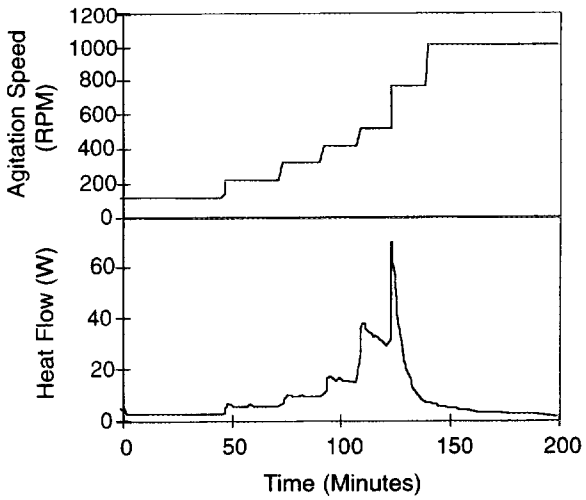


FIG. 2. Heat flow as a function of agitation speed for the hydrogenation of pyrazine-2-*tert*-butylcarboxamide (**I**) over a 5% Pd/C catalyst at 1 *M* initial substrate concentration, 0.0038 (wt/wt) Pd/substrate, 343 K, 593 kPa.

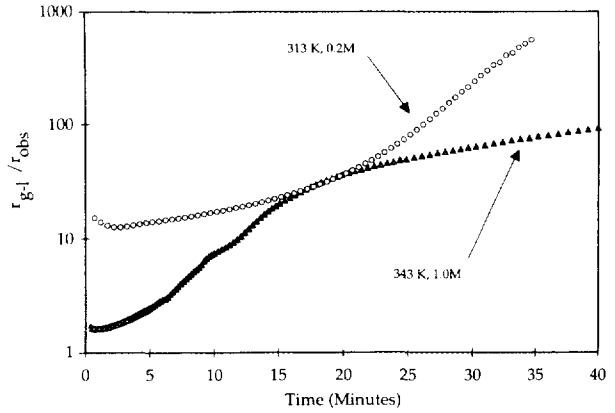


FIG. 3. Ratio of the maximum rate of gas–liquid mass transfer ($r_{g\ l}$) to the observed rate of reaction ($r_{obs}$) as a function of reaction time for reactions carried out under different conditions over a 5% Pd/C catalyst: (a) 343 K, 593 kPa, 1.1 *M* initial substrate concentration 0.0038 (wt/wt) Pd/substrate; (b) 313 K, 663 kPa, 0.2 *M* initial substrate concentration, 0.00095 (wt/wt) Pd/substrate.

lated from Eq. [4] may then be compared to the rate of hydrogen consumption measured during the hydrogenation reaction at 1000 rpm. It has been suggested that a tenfold ratio between the rate of transferring hydrogen into the liquid to the rate at which it is consumed in the reaction is sufficient to insure that the reaction will be free from gas–liquid mass transfer limitations. Figure 3 plots this ratio of rates over the course of the reaction carried out at high and low initial substrate concentrations. The rate of reaction in terms of moles hydrogen consumed/liter/min was calculated from the experimental heat flow curve and the hydrogen uptake during the reaction. For the higher temperature and initial substrate concentration, the initial reaction rate was very close to the hydrogen gas–liquid mass transfer rate, confirming the severe diffusion limitations intimated by the results in Table 1 and Fig. 1 for similar reaction conditions. It should also be noted, however, that gas–liquid mass transfer of hydrogen ceased to be the controlling step as the reaction progressed and the hydrogen consumption rate decreased concomitant with the decrease in the substrate concentration driving force.

Figure 3b shows this ratio of rates for the reaction carried out at the lower temperature of 313 K and using lower substrate and catalyst concentrations, all parameters which in effect provided a lower initial reaction rate. Under these conditions it is clear that the entire course of the reaction took place outside the mass transfer controlled regime. Thus several simple measurements have been combined to delineate clearly how reaction conditions under which gas–liquid mass transfer is the controlling rate may be avoided. Heat flow as a function of agitation speed provided an intuitive picture of gas–liquid mass transfer and measurements of $K_La$ provided quantitative corroboration of the controlling regime.

It should be noted that our study addresses only gas–liquid diffusion and that other rate processes which might interfere with the measurement of intrinsic kinetics, such as liquid–solid transport and pore diffusion resistances, were not investigated in our work; although other studies have investigated how these rate processes may be monitored (12).

### *Kinetic Modeling*

The reactions described thus far have focused on total, or nonselective, hydrogenation of the pyrazine substrate to produce a racemic mixture of the product **IV**, which contains a chiral carbon at the substituted 2 position in the ring. However, if the partially hydrogenated species **III** could be produced in high yield, it might serve as a substrate for attempting enantioselective hydrogenation in a separate step over a chiral catalyst to produce the desired (*S*)-piperazine-2-*tert*-butylcarboxamide. We therefore sought to explore how calorimetric measurements could

TABLE 2

**Gas–Liquid Mass Transfer Coefficients**

| Solution | $H_2$ solubility ($M \times 10^2$) | Gas–liquid mass transfer coefficient, $K_La$ ($s^{-1}$) | | Maximum rate of gas–liquid mass transfer (mmoles $H_2$/liter/min) | |
|---|---|---|---|---|---|
| | | 400 rpm | 1000 rpm | 400 rpm | 1000 rpm |
| @ 293 K | 1.16 | 0.0022 | 0.227 | 1.53 | 103.8 |
| 40 g/liter **I**/PrOH @ 333 K | 1.30 | 0.0044 | 0.48 | 3.64 | 350 |
| 200 g/liter **I**/PrOH @ 343 K | 1.44 | 0.0029 | 0.68 | 2.54 | 554 |

help to delineate reaction conditions for carrying out the selective hydrogenation to intermediate products in such a hydrogenation reaction network.

*Heats of reaction.* Before choosing a kinetic model to describe the reaction rates in Eq. [1], we carried out molecular modeling to provide estimates for the heat of reaction of each step in the network as described in the Experimental Section. The most stable structures for intermediates **II** and **III** were predicted by molecular modeling to be:

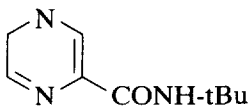


**II**

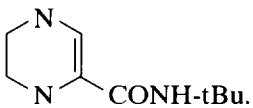


**III**

Compound **II** was unstable in air, oxidizing readily back to **I**, but the proposed structure for compound **III** was confirmed experimentally by $^{13}$C-NMR (13). Standard heats of reaction for reactions 1, 2, and 3 were estimated to be −9.9, −17.7, and −20.6 kcal/mol, respectively. The first step in the hydrogenation network involves both the hydrogenation of a C=N bond, releasing 22 kcal/mol, and removal of the resonance energy of the substituted pyrazine ring. The reported resonance energy for pyrazine itself is 22.3 kcal/mole (14), helping to rationalize why the first step is considerably less exothermic than the second and third hydrogenation steps. As a comparison, hydrogenation of benzene involves a first step which is thermodynamically unfavorable by 5.6 kcal/mole, due to the higher resonance energy of benzene (36 kcal/mol) compared to pyrazine (15).

The last two steps exhibited similar heats of reaction, both considerably higher than the first step due to the removal of the aromaticity in the first step. The heat of reaction for the entire consecutive reaction sequence was estimated by the model to be −48.2 kcal/mol, which is in good agreement with our experimentally determined value of −44 kcal/mol as well as with the value of 48.1 kcal/mol obtained from the literature for pyrazine (15).

*Kinetic studies.* We chose to model the hydrogenation sequence as a three-step series of first-order reactions. Although this choice may appear to be simplistic for describing a complex organic reaction occurring over a solid metal catalyst, it provides us with an example to compare calorimetric data with kinetic data obtained from more conventional analytical methods. Isothermal reactions were carried out between 293–313 K at a substrate molarity chosen to insure the absence of gas–liquid mass transfer limitations. Heat flow curves from each reaction were used to solve Eq. [7] for kinetic parameters as described in the Experimental Section. It is useful to emphasize that a simple experimental heat flow curve contains embedded in it all of the information necessary to determine the concentration of all of the species in the reaction network, provided that reasonable estimates of heats of reaction are available and that valid kinetic expressions of the reaction rates are used.

TABLE 3

**Reaction Parameters from Molecular Modeling and from Heat-Flow-Derived Kinetic Model**

| Reaction | Preexponential factor units ($10^{8} \times s^{-1}$) | Activation energy (kcal/mol)[a] | Heat of reaction (kcal/mol)[b] |
|---|---|---|---|
| **I** → **II** | 7.96 | 13.9 | 9.9 |
| **II** → **III** | 8.83 | 13.8 | 17.7 |
| **III** → **IV** | 0.09 | 12.6 | 20.6 |

[a] From heat-flow-derived first-order kinetic model (see Experimental Section for details). Catalyst = ES-5 (see Table 1); surface specific reaction rate in moles substrate/moles surface Pd/s or $s^{-1}$.

[b] From molecular modeling (see Experimental Section for details).

Table 3 gives the first-order model-derived values of $A_i$'s and $E_{a,i}$'s as well as the $\Delta H_{rxn,i}$'s derived from molecular modeling. Figure 4 compares the experimentally measured heat flows with those generated by the first-order consecutive model described above. These values represent the best solution (average percent error <7%) obtained given a range of reasonable initial guesses for the parameters, but, as discussed in the Experimental Section, the solution may not represent a global minimum. At all three temperatures, the model correctly predicts the initial concave-downward shape characteristic of the consecutive reaction network, but it has difficulty at lower temperature in correctly positioning the maximum in heat flow. At high con-

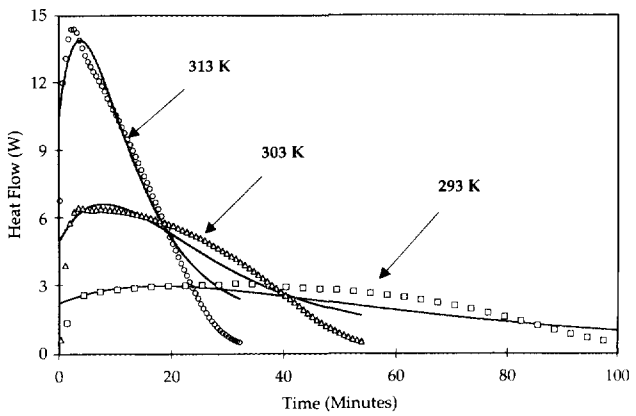


FIG. 4. Heat flow as a function of reaction time for the isothermal hydrogenation of **I** over a 5% Pd catalyst at 0.2 *M* substrate concentration, 0.00095 (wt/wt) Pd/substrate, 593 kPa. Comparison of model fit (-----) with experimentally obtained heat flow data (symbols).

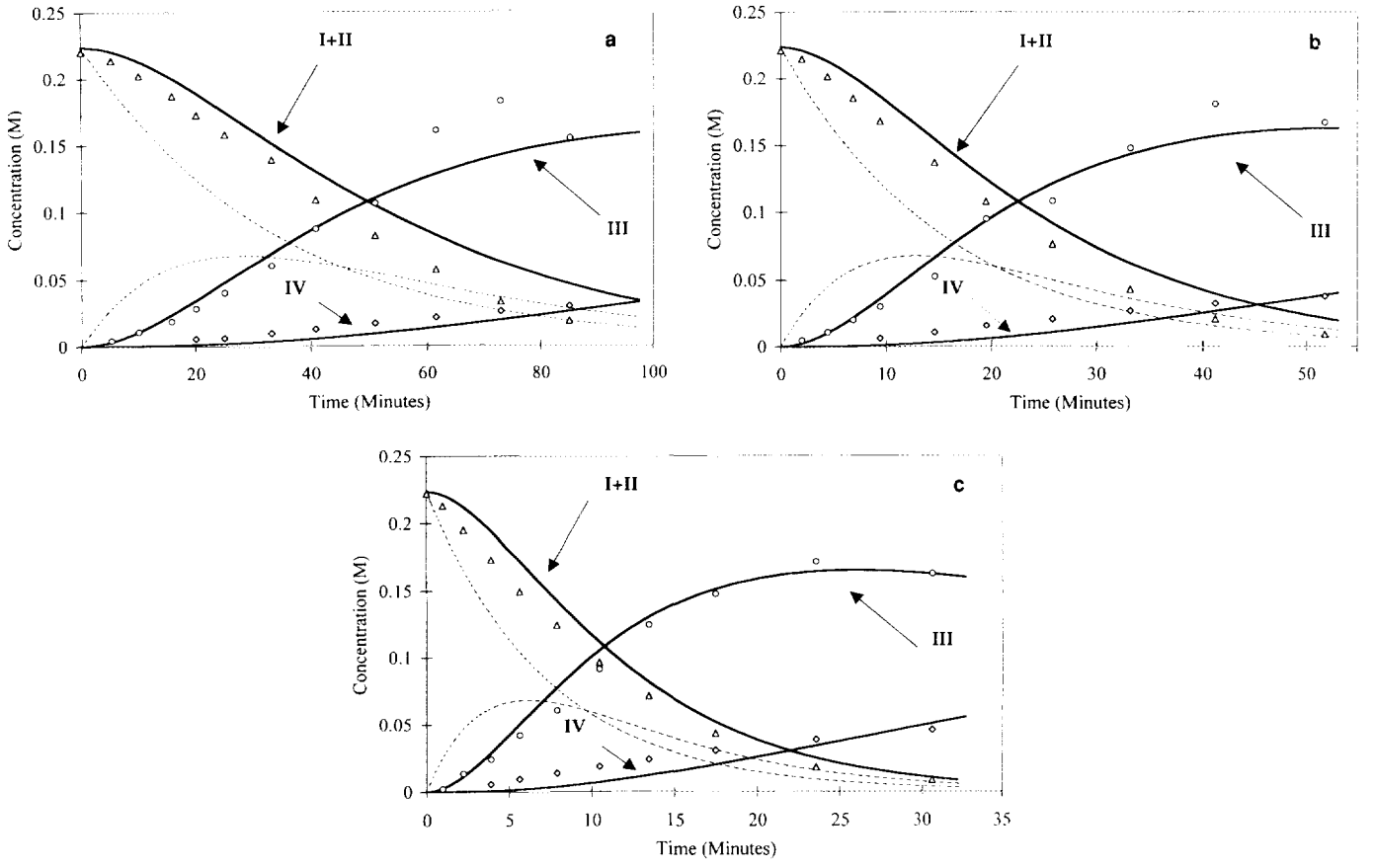


FIG. 5. Concentration of reactant, intermediates, and product as a function of reaction time for the isothermal hydrogenation of **I** over a 5% Pd catalyst at 0.2 *M* substrate concentration, 0.00095 (wt/wt) Ps/substrate, 487 kPa. Symbols are experimental data points from LC analysis for species **I** + **II** (△) and **III** (○); GC analysis for **IV** (◇). Bold lines are concentration profiles predicted from the heat flow kinetic model for each species as marked. Dashed lines are for the model-derived concentrations of species **I** and **II** separately: (a) 293 K; (b) 303 K; (c) 313 K.

version in each case the model overpredicts the heat flow generated (i.e., the reaction rate). It is likely that a more complex model than the simple first-order model employed may better represent the reaction network, or that the kinetic parameters are not constant over the temperature range studied. This could be observed if a change in mechanism occurred over the temperature range studied, or if rate processes other than intrinsic kinetics, such as pore diffusion, contributed to the observed rate.

An important question to be addressed even given these shortcomings is whether the fit achieved with this simple model is accurate enough to be of use in predicting species concentrations over the course of the reaction at various temperatures. To help address this point, the reaction mixture was also sampled periodically throughout each reaction. The concentration data we obtained directly may be compared to those we predicted from the heat flow curve and Eq. [7], as shown in Figs. 5a–5c, where the solid lines represent concentration profiles as calculated from the heat-flow-derived model compared to actual data points for concentration of species **I** + **II**, **III**, and **IV**. It is clear from these plots that the heat flow model is quite successful in tracking the concentration profiles of these species. In fact, in one instance the heat flow model provides information that analytical methods failed to give: the model allows us to follow species **II** separately from species **I**, a result which would not have been possible if analytical sampling had been our only tool, due to the instability of **II** as was discussed earlier.

As was implied from the fit of the experimental heat flow curves themselves, however, the first-order model is probably not an accurate description of the kinetics of this reaction network over the entire temperature range chosen, and the kinetic parameters derived from it must be regarded as estimates. For example, the activation energies provided by the kinetic model are similar for each step in the sequence while intuition would predict a higher activation energy for the third step to rationalize the observed buildup of species **III**. A higher $E_{a\mathbf{III}}$ value in this model would compensate with a lower, and physically less

realistic, value for $A_{0III}$. Further refinements in the modeling would require development of a more complex kinetic expression for the consecutive reaction network.

However, even given these limitations, the model provided conclusions which can be valuable in directing the course of future experimental work on this reaction network: high yield to species **II** is unlikely to be achieved under any conditions; the intermediate species **III** can indeed be produced in high yield if low enough reaction temperatures are employed; and, as expected, high temperature should be used if total hydrogenation of the pyrazine ring to **IV** is required. Even with the simple model chosen here, it is clear that kinetic modeling using global heat flow measurements can be combined with species-specific analytical measurements to test the predictive power of the model, thus making use of two independent measures of reaction progress. In kinetic studies where sample analysis provides the only source of information about reaction kinetics, a "good" fit to a model does not necessarily lend assurance that the kinetic parameters obtained are physically meaningful since the data provides merely a fit and not a test of the kinetic model. Hence calorimetry can provide a valuable tool to aid in the description of complex catalytic reaction networks.

## CONCLUSIONS

Heat flow calorimetry has been demonstrated as an effective tool in developing a simple kinetic picture of a complex catalytic reaction network. Heat flow measurements were used as a rapid test of bulk diffusion limitations. In the absence of such limitations, monitoring the heat flow over the course of the reaction provided a global measure of the reaction progress which could be deconvoluted to predict trends in the concentration profiles for all species in the consecutive reaction network. Using heat flow as a measure of reaction progress provided a measure of species concentrations completely independent from analytical sampling. The utility of combining independent measurements of reaction progress as a means of assessing kinetic models was discussed.

## REFERENCES

1. Guisnet *et al.*, Eds., "Heterogeneous Catalysis and Fine Chemicals Synthesis." Elsevier, Amsterdam, 1991; "Catalysis of Organic Reactions." M. G. Scaros and M. L. Prunier, Eds., Dekker, New York, 1994.
2. Roberts, G. W., *in* "Catalysis in Organic Synthesis 1976," (P. N. Rylander and H. Greenfield, Eds.), p. 1. Academic Press, New York, 1976.
3. Singh, U. K., Landau, R. N., Sun, Y., LeBlond, C., Blackmond, D. G., Tanielyan, S. K., and Augustine, R. L., *J. Catal.* in press.
4. Askin, D., Eng. K. K., Rossen, K., Purick, R. M., Wells, K. M., Volante, R. P., and Reider, P. J., *Tetrahedron Lett.* **35,** 673 (1994).
5. Pearlman, W. M., *Tetrahedron Lett.* **17,** 1665 (1967).
6. Matsumara, M., Masunaga, H., and Kobayashi, J., *J. Ferment. Technol.* **57,** 107 (1979).
7. Deimling, A., Karandikar, B. M., Shah, Y. T., and Carr, N. L., *Chem. Eng. J.* **29,** 140 (1984).
8. Landau, R. N., and Blackmond, D. G., and Tung, H.-H., *Ind. Eng. Chem. Res.* **33,** 814 (1994).
9. Landau, R. N., and Blackmond, D. G., Chemical Engineering Progress, Nov. 1994, p. 43.
10. Dewar, M. J. S., Zoebisch, E. G., Healy, E. F., and Stewart, J. J. P., *J. Am. Chem. Soc.* **107,** 3902 (1985).
11. Daly, F. P., Jensen, W. M., and Ostgard, D. J., *in* "Catalysis of Organic Reactions" (M. G. Scaros and M. L. Prunier, Eds.), p. 13. Dekker, New York, 1994.
12. Garland, M., Jalett, H. P., and Blaser, H. U., *in* "Heterogeneous Catalysis and Fine Chemicals II" (Guisnet *et al.*, Eds.), p. 177. Elsevier, Amsterdam, 1991.
13. Reamer, R., unpublished results.
14. Häfelinger, V. G., and Steinmann, L., *Angew. Chem.* **89,** 48 (1977).
15. Streitwieser, A., Jr., and Heathcock, C. H., (Eds.), *in* "Introduction to Organic Chemistry" 3rd ed., p. 564. Macmillan Co., New York, 1985.